High-Efficiency Distortion-Free Delivery of 3 kW Continuous-Wave Laser Using Low-Loss Multi-Mode Nested Hollow-Core Anti-Resonant Fiber

Jingyuan Yao, Xin Zhang, Biao Li, Beibei Wang, Dongchen Jin, Yunfeng Duan, Juyun Zhao, and Pu Wang

***Abstract*—Hollow-core anti-resonant fibers (HC-ARFs) are widely used for high-power laser transmission owing to their low nonlinearity and high damage threshold. However, most existing structural designs are suitable for single-mode guidance but are inadequate for efficient transmission of few- or multi-mode lasers with high output power. In this study, we fabricated a low-loss multi-mode 8-tube nested hollow-core anti-resonant fiber (Nested HC-ARF) with a minimum loss of 3.27 dB/km at 1 μm wavelength, which enabled the efficient transmission of at least five mode groups. Accordingly, we demonstrated the transmission of a record 3 kW few-mode ($M^2 \sim 1.38$) continuous-wave laser with a maximum transmission efficiency of 95.2% using a 10 m multi-mode Nested HC-ARF and an optimized transmission system. The experimental verification of the beam quality and spectrum indicated distortion-free transmission, which paves the way to power delivery on the scale of tens of kilowatts.**

***Index Terms*—High power laser, hollow core fiber, laser flexible transmission, multi-mode.**

I. Introduction

THE performance of high-power lasers has rapidly improved over the years. Consequently, high-power lasers have become instrumental in the development of industrial processes [1] and national defense technologies [2]. Although researchers are attempting to further improve the output power of high-power lasers, inefficient transmission methods have limited the widespread application of high-power lasers. Free-space transmission introduces complex spatial optical paths, resulting in insufficient flexibility and stability. Therefore, the demand for high-power laser transmission based on flexible fibers is increasing. Traditional solid silica fibers are available for such applications [3], transmission of 1 kW of power over 300 m [4] and 10 kW over 30 m [5] have been demonstrated in a three-mode photonic crystal fiber. Commercially available solutions are typically limited to a few 10s of meters e.g., a commercial multi-mode 10 kW fiber laser has 100 μm diameter delivery fiber up to 30 m long [6]. Despite these achievements, the damage threshold and material nonlinearity eventually affect them, thereby limiting the increase of transmission power and length [7], [8].

Hollow-core fibers [9], especially hollow-core anti-resonant fibers (HC-ARFs) [10], [11], [12], [13], provide novel solutions for flexible high-power laser transmission by guiding light through air, vacuum, or gas-filled hollow core. Compared to solid-core fibers, HC-ARFs inherently reduce the overlap between the optical field and glass structure to 5 orders of magnitude lower [12], [14], resulting in low optical nonlinearity [15] and a higher damage threshold [16]. Recently, numerous multilayer structures have emerged based on the knowledge of light-guiding mechanisms, which rapidly decrease the loss of HC-ARFs [17], [18], [19], [20], [21]. The unique properties of these innovatively structured HC-ARFs offer significant potential in terms of transmission distance, flexibility, and power-handling capacity.

The rapid development of HC-ARF technology has resulted in successful practical demonstrations of laser power delivery through HC-ARFs, particularly at a wavelength of 1 μm. Until now, laser power delivery systems with kilowatt-scale average power [22], [23], pulse energy up to 30 mJ [24], and peak power of 1.4 GW [25] have been reported. In particular, the breakthrough result of transmitting 1 kW of power over a 1 km long low-loss Nested HC-ARF indicates that the unique properties of HC-ARFs significantly improve the laser power delivery [22]. This has been further validated by the recent transmission of a 2.2 kW high-brightness narrow-linewidth laser by Nested HC-ARF [23]. Most existing studies have focused on achieving superior performance while maintaining efficient single-mode operation, which validates the excellent characteristics of laser transmission using HC-ARFs. However, for lasers with higher

Manuscript received 10 January 2024; revised 12 March 2024 and 17 April 2024; accepted 7 May 2024. Date of publication 13 May 2024; date of current version 16 August 2024. This work was supported in part by the National Natural Science Foundation of China under Grant 62035002, Grant 62305014, and in part by "Yeqisun" Science Foundation under Grant U2241225. *(Corresponding authors: Pu Wang; Xin Zhang.)*

Jingyuan Yao, Xin Zhang, Biao Li, Beibei Wang, and Pu Wang are with the Institute of Laser Engineering, Faculty of Materials and Manufacturing, Beijing University of Technology, Beijing 100124, China (e-mail: yaojy@emails.bjut.edu.cn; zhangxin940425@bjut.edu.cn; antik0814@163.com; wangb@emails.bjut.edu.cn; wangpuemail@bjut.edu.cn).

Dongchen Jin, Yunfeng Duan, and Juyun Zhao are with the BWT Tianjin Ltd., Tianjin 300000, China (e-mail: jindongchen@bwt-bj.com; duanyunfeng@bwt-bj.com; yunkai@bwt-bj.com).

Color versions of one or more figures in this article are available at https://doi.org/10.1109/JLT.2024.3400293.

Digital Object Identifier 10.1109/JLT.2024.3400293

output powers and a wide range of applications, maintaining the single-mode operation can be challenging, as they typically have few- or multi-mode outputs [26]. Existing low-loss HC-ARFs are predominantly effective for single-mode transmission, but they exhibit extremely high losses in higher-order modes [27], [28]. This results in a substantially low efficiency for few- or multi-mode laser transmission and hinders the increase in transmission power.

Several studies have reported theoretical simulations of multi-mode HC-ARFs intended for reducing the transmission loss in higher-order modes or for increasing the number of modes that can be transmitted at a low loss [29], [30], [31]. These designs typically enable low-loss transmission in 5-8 mode groups. In terms of laser transmission [6], multi-mode HC-ARFs have been designed depending on the beam quality of the incident laser that could achieve a coupling efficiency of over 95%. These designs require precise control of the thicknesses of multiple glass interfaces in the radial direction during fabrication and care to avoid structural deformation due to contact between neighboring capillaries. At the same time, the supporting silica rods or struts in some of these structures further complicate the molding of the fibers. Consequently, little work has been reported on the practical fabrication of these high-performance multimode HC-ARF designs. For successfully fabricated multi-mode HC-ARFs, Winter et al. [32] fabricated a single-ring HC-ARF with a core diameter of 164 μm, guiding approximately 10 modes. The attenuation of this fiber was approximately 0.1 dB/m. Although other multi-mode HC-ARFs [33], [34] were subsequently fabricated, their losses were considerably high for practical applications. Overall, high-performance multi-mode HC-ARFs are currently lacking in the field of laser delivery.

In addition, high-power lasers produce severe thermal lensing effects on the coupling optics, which limit the further increase in the transmission power of HC-ARFs. In the spatially coupled approach, thermal deflection due to thermal lensing effects reduces the transmission efficiency [35]. This can lead to significant optical power leakage and burn the fiber, thus limiting the increase in transmitted power. Additionally, owing to the mismatch between the Gaussian beam and mode field of the HC-ARF [36], the power lost at launch, which is not coupled to the core, is likely to heat and damage the fiber end-face or cause absorption by the coating, resulting in fiber failure. Therefore, the thermal management of lenses and fibers is crucial. In conclusion, the power improvement of HC-ARF transmission systems is limited by the challenges in the fabrication of high-performance multi-mode HC-ARFs and the thermal management ability of lenses and fibers during transmission.

To address the aforementioned issues, in this study, we fabricate a low-loss multi-mode 8-tube Nested HC-ARF with a minimum loss of 3.27 dB/km at a wavelength of 1 μm. We demonstrate the transmission of a 3 kW few-mode continuous-wave laser based on our 10 m multi-mode Nested HC-ARF with a maximum transmission efficiency of 95.2%. To the best of our knowledge, this is the highest reported transmission power achieved using HC-ARF. The resulting beam quality and spectrum are found to be in good agreement with those of the laser source.

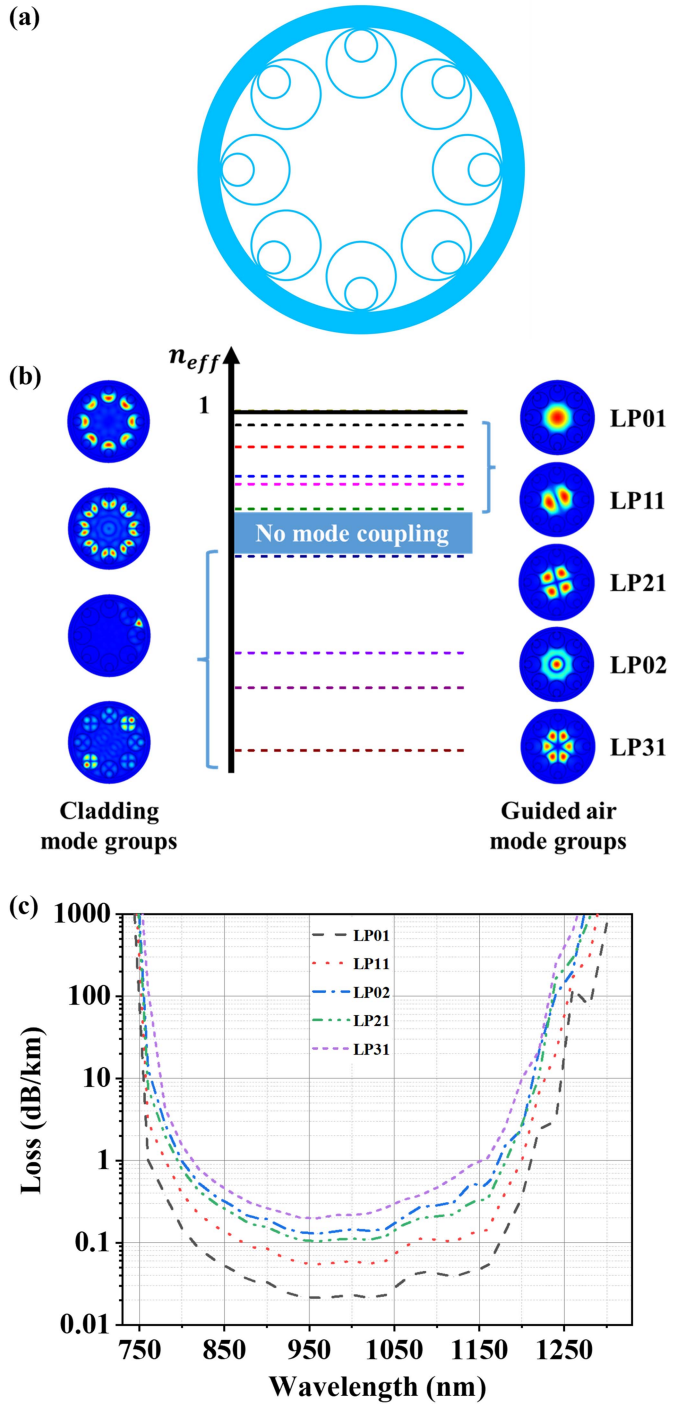

Fig. 1. (a) Geometric structure of the designed 8-tube multi-mode nested hollow-core anti-resonant fiber (Nested HC-ARF). (b) Simulation results of the effective refractive index distributions of modes. (c) Simulated loss spectra of five scalar modes in the fiber.

II. Fabrication and Characterization of Low-Loss Multi-Mode Nested HC-ARF

Although HC-ARF with a larger core size supports a multitude of air-guided modes, its guidance mechanism introduces a large differential loss between them [12]. The higher-order modes experience higher leakage losses than the fundamental modes and are prone to resonant coupling with the air modes

in the cladding microstructure, which accelerates optical losses. To achieve a stable multi-mode transmission, we designed an 8-tube Nested HC-ARF with a core diameter of 65 μm and an average gap of 4.8 μm between the nested tubes, as shown in Fig. 1(a). The nested tube thickness is 700 nm, and the outer diameter ratio of the inner and outer tubes is 0.475.

The design principles are as follows. First, a nested tube structure was used to reduce the leakage loss of the core guidance mode. Subsequently, by adjusting the number and the proportion of the nested tubes, a large separation was induced in the effective index between the core and cladding modes to form a phase mismatch. The simulations were performed using a finite-element mode solver (COMSOL Multiphysics) with optimized mesh size and perfectly matched layer [37]. As shown in Fig. 1(b), the effective refractive index distributions of the LP_{01}, LP_{11}, LP_{21}, LP_{02}, and LP_{31} mode groups in the fiber core ranged from 0.99993 to 0.99949, significantly exceeding that of the cladding modes (starting at 0.99924). As the effective refractive index spacing between the core modes and the cladding modes are larger than $\Delta n_{eff} = 10^{-4}$ [38], this effectively prevents the energy coupling of the mode groups with the cladding mode and achieves low-loss multi-mode transmission in the fiber. We analyzed the loss properties of these five mode groups in the fiber core. Fig. 1(c) depicts the average loss of each mode group. Micro-bending loss, as an external loss mechanism of hollow core fiber, is closely related to process parameters such as cladding diameter, coating characteristics, and winding scheme [19], so we included only the confinement and scattering losses to evaluate the mode loss [12]. The simulation results indicated that the fundamental mode losses were 0.022, 0.034, and 0.044 dB/km at 1030, 1060, and 1080 nm, respectively. Although the general trend indicated that the loss increased with the order of the mode, the differential mode losses were mitigated under a large core size and multi-layer design. The losses of all 16 core modes were less than 1 dB/km in the wavelength range of 810–1150 nm, and the maximum mode loss ratio among them did not exceed 10. This validated the capability of the fiber to support low-loss multi-mode transmission.

Based on the designed structure, we fabricated a multi-mode Nested HC-ARF using the stack-and-draw method. The complex multi-layer structure and relatively large ratio of the core size to the thickness of the nested tube render the fiber cross-section susceptible to distortion during fabrication. To obtain the required fiber geometrical sizes, multiple independent pressures were carefully applied to different areas of the fiber, combined with a relatively low furnace temperature and extremely high drawing tension. Fig. 2(a) shows a scanning electron microscopy (SEM) image of the 217 m long multi-mode Nested HC-ARF. The stable fabrication process makes the cross-section of this length of fiber almost indistinguishable between the head and tail end. Eight nested tubes were attached to the inside of the glass-jacket tube along the angular direction to form an air core with a diameter (*ID*) of 65 μm at the center of the distribution. The average diameters of the outer (*D*) and inner (*d*) nested tubes were 30.1 and 13.6 μm, respectively. The maximum, minimum, and average wall thicknesses of the outer tube were 690 nm, 667 nm, and 675 nm, while for the inner tube these parameters were

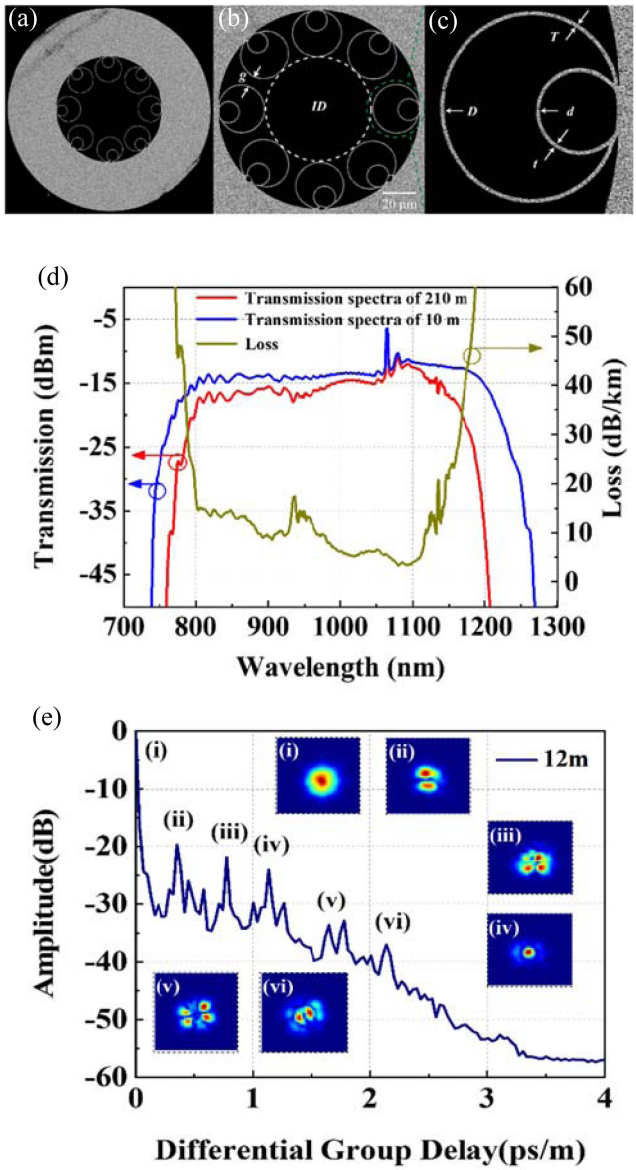

Fig. 2. (a) Scanning electron microscopy (SEM) image of the fabricated nested hollow-core anti-resonant fiber (Nested HC-ARF). (b) and (c) Terms used for defining the structure. (d) Measured transmission spectra and the evaluated cutback loss (lower curve) of the 210 m long (upper curve) and 10 m long (middle curve) Nested HC-ARF under identical launch conditions. (e) Differential group delay plot based on the spectral and spatial (S^2) measurements using the 12 m long fiber. The inset images depict the reconstructed mode profiles (i–vi).

707 nm, 659 nm, and 680 nm, respectively. These nested tubes were uniformly arranged with an average gap (*g*) of 5.8 μm. Our Nested fiber was coated with a high refractive index single-layer coating to improve the mechanical strength of the fiber. The diameters of the fiber before and after coating are 230 μm and 380 μm, respectively.

The multi-mode Nested HC-ARF was spooled on a 1 m circumference bobbin (16-cm-radius) during the fabrication process. Consequently, its attenuation was characterized using the cut-back method without any rewinding treatment. A supercontinuum (SuperK Compact, NKT Photonics) was connected to an SMF-28 fiber and butt-coupled to the tested Nested HC-ARF,

and the output was connected to an optical spectrum analyzer (AQ6370C, Yokogawa) using a bare-fiber adaptor. The input end of the Nested HC-ARF was unaltered, and the cut-back measurement was applied to the fiber length, which decreased from 210 to 10 m. For multimode fiber, it was difficult to accurately characterize the loss of each mode by cut-back method. Therefore, we maximized the excitation of the fundamental mode of fiber and measured its loss. The modal content at the output of a 10 m length of the Nested HC-ARF was subsequently measured using the spectral and spatial (S^2) imaging technique [39]. The fraction of power in the fundamental mode was greater than 95%. The reliability of the measurements was ensured by recording four separate transmission traces from four different cleaves of the Nested HC-ARF output end for different fiber lengths. Fig. 2(d) shows the measured transmission spectra and attenuations of the fabricated fibers obtained using the cut-back method. The Nested HC-ARF transmitted across the wavelength range of 950–1207 nm with a minimum loss of 3.2 dB/km at 1080 nm The loss was lower than 10 and 20 dB/km across the wavelength ranges of 967-1117 nm and 799-1144 nm (bandwidth of 345 nm), respectively. The attenuation of the fabricated multi-mode Nested HC-ARF was higher than expected. This is due to the relatively large core to wavelength ratio [19], which results in macro-bending and micro-bending loss in the wavelength range of 799-1207 nm. Moreover, the slight deformation caused by the rotation of the partially nested tube resulted in additional optical leakage. Even so, the loss of our fabricated multimode HC-ARF is reduced by two orders of magnitude compared to the previously fabricated multimode HC-ARF [32], [34]. In addition, the loss characteristics of the fiber were sufficient for high-power laser transmission fields, which use fiber lengths ranging from several to tens of meters.

The modal content of the fabricated fiber was characterized using spectral and spatial (S^2) imaging techniques in the wavelength range of 1075–1085 nm to verify its multi-mode transmission properties. The optical source used was the same supercontinuum light source mentioned above, and its pigtail was butt-coupled to the Nested HC-ARF being tested. The length of the tested Nested HC-ARF was 12 m with a bending diameter of 40 cm. Owing to the large mode field mismatch between the pigtail and the Nested HC-ARF, a certain amount of higher-order mode components were excited during butt-coupling [6]. Fig. 2(e) shows the differential group delay of the fiber. Seven peaks are observed between 0 and 4 ps/m. In addition to the fundamental mode, higher-order modes such as LP_{11}, LP_{21}, LP_{02}, LP_{31}, and LP_{12} are evident (corresponding reconstructed mode profiles are shown in Fig. 2(e)i–vi). The experimental results confirm the multi-mode transmission characteristics of the fabricated fiber.

III. High Power Laser Delivery Demonstration

Fig. 3(a) shows the experimental setup of the high-power continuous-wave laser delivery system. In this experiment, a commercial fiber laser (BWT) was used as the continuous-wave laser source. It provided a maximum power of 3100 W at 1080 nm with a beam quality factor of $M^2 = 1.38$, thus indicating

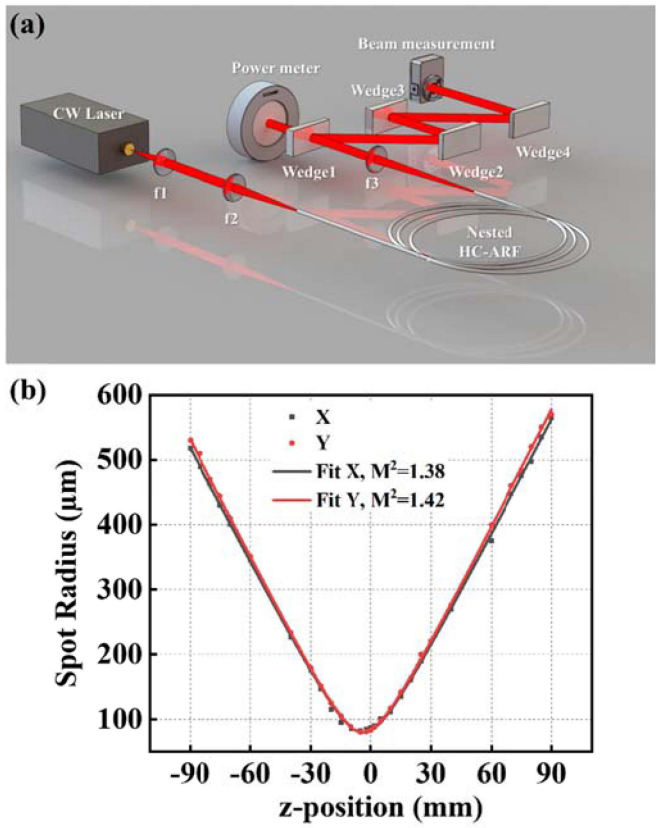

Fig. 3. (a) Experimental setup of the power transmission system. (b) Beam quality factor measurements for the 10 m long nested hollow-core anti-resonant fiber (Nested HC-ARF) at a low output power of 38 W.

a few-mode output. The laser output beam was collimated using a plano–convex lens. Selected another suitable plano-convex lens to match the focused spot size to the MFD of Nested HC-ARF. The tested fiber was placed on a three-axis stage and the lenses were placed on the five-axis stages to achieve precision alignment. In order to achieve high coupling efficiency, the output power was monitored in real time and maximized by precise adjustment of the alignment. The output spot profile was also monitored to ensure that it was not distorted. The high coupling efficiency avoided the potential burning of the fiber coating caused by the leaking of light that is not guided into the core. Thermal lensing effects in coupling optics caused by absorption at high powers result in focal shifts and beam distortions [35]. In the proposed experimental setup, high-purity fused silica was used as the material for the convex lens to minimize laser absorption.

We loosely coiled a 10 m long Nested HC-ARF on an optical platform with a bend radius of 30 cm to prevent the generation of bending loss. The input and output of the Nested HC-ARF were precisely cleaved using LDC400. The first 15 cm of the fiber was stripped from the coating and placed in a water-cooled V-groove. The length of the V-groove was 10 cm. Fig. 3(b) shows the beam quality factor of the Nested HC-ARF measured with a beam profiler (Thorlabs BP209-VIS) at a low output power of $P_{out} = 38$ W. The measurement resulted in M^2 values of 1.38 $\pm$ 0.02 and 1.42 $\pm$ 0.02 for the horizontal (x) and vertical (y)

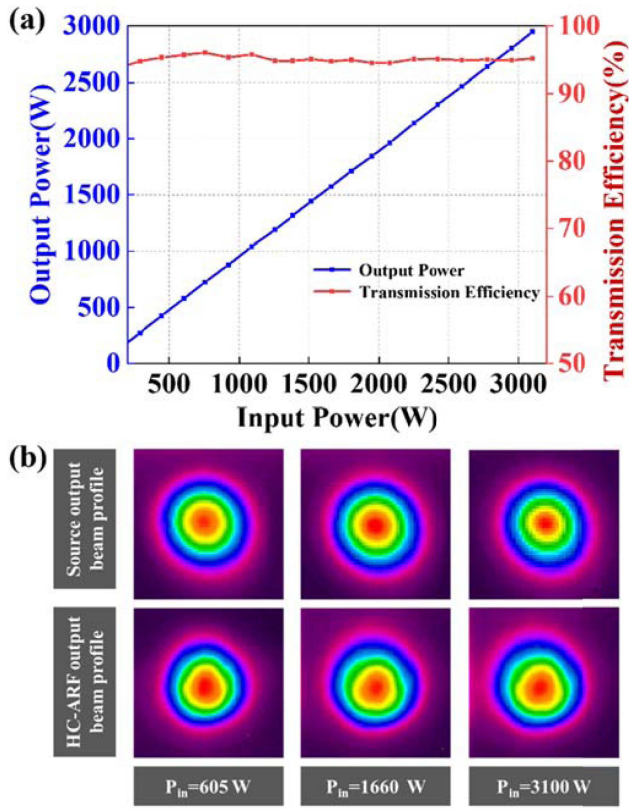

Fig. 4. (a) Power-delivery performance of the 10 m long nested hollow-core anti-resonant fiber (Nested HC-ARF). Left axis: Nested HC-ARF output power versus the nested HC-ARF input power. Right axis: Throughput efficiency. (b) Near-field beam profiles of the laser beam (upper row) and Nested HC-ARF output beam at three input power levels of P_{in} = 605, 1660, and 3100 W.

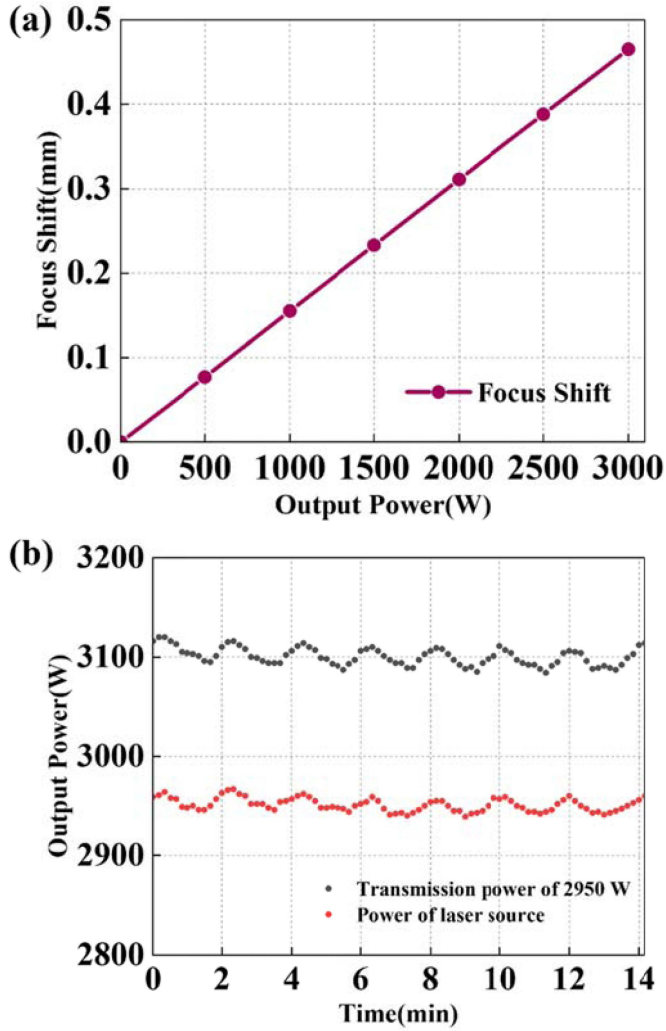

Fig. 5. (a) Focal shift versus the input power of the nested hollow-core anti-resonant fiber (Nested HC-ARF). (b) Power stability of the laser source at a transmission power of 2950 W.

directions, respectively, hence indicating that the beam-quality factor can be maintained at the same level as that of the laser source for a transmission length of 10 m. The increase in M^2 of the output beam in the vertical direction is due to fiber bending.

Fig. 4(a) shows the high-power delivery results via a 10 m long Nested HC-ARF, where the left and right axes denote the output power of the Nested HC-ARF and the corresponding transmission efficiency, respectively. When the power at the laser source was 3100 W, the maximum output power was 2950 W. The total transmission efficiency (TE = Pin / Pout) was 95.2%, which included the coupling efficiency and the 10 m long fiber transmission loss. The high coupling efficiency implies that the majority of the mode contents of the laser source are transmitted by the 8-tube Nested HC-ARF. In previous research [22], [23], a laser with near diffraction-limited output was required for efficient transmission. Instead, we used a multi-mode HC-ARF to achieve high-efficiency transmission for a laser with less-than-perfect beam quality. The transmission efficiency stabilized as the laser power increased. The temperatures of the fiber ends and coating were 54.8°C and 39.8°C, respectively, which were substantially below the damage threshold. Although the power can be increased further, it is currently limited by the maximum output power of the laser source.

Considering experimental safety and the influence of attenuating optics on the measurement results, the beam quality of the Nested HC-ARF was not measured at higher powers. Instead, we monitored the beam profile of the output at different powers and compared it with that of the laser (Fig. 4(b)). The near-field beam profile was imaged using a charge-coupled device camera connected to Spiricon beam profiling software. We attenuated the power of the output beam through multiple wedges to meet the testing requirements. No significant changes were observed in the beam profile with an increase in the input power. In summary, the beam profile remained constant, and the transmission efficiency remained considerably high. Therefore, we can infer that no significant change in the output beam quality factor occurs as the input power increases.

It is noteworthy that during high-power laser transmission, to avoid a decrease in the transmission efficiency, the focus shift caused by the thermal lensing effect needs to be adjusted for the coupling position with an increase in the input power. To maintain the coupling efficiency at high power levels and

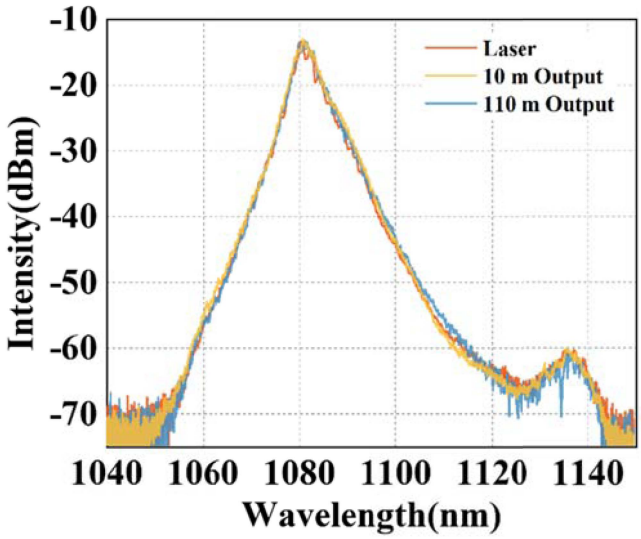

Fig. 6. Measured input and output spectra at fiber lengths of 10 m and 110 m at P_{in}= 3100 W.

avoid burning the fibers, we simulated the thermal lensing effect using COMSOL Multiphysics 5.6 software to determine the focal change at different transmission powers (Fig. 5(a)). The simulation results were in good agreement with the focus shift at the highest power measured in our experiments. During the experiment, the focus shift was calculated in advance by simulating the thermal lens effect, pre-compensating for focus before an increase in power. Consequently, the adjustment of the fiber position could be avoided during high-power laser transmission to maintain high transmission efficiency.

The stability of a transmission system is another important indicator of its performance. Therefore, we obtained the measurements corresponding to the stability of the system. Fig. 5(b) illustrates the transmission stability that was recorded for 14 min at the maximum output power. The fluctuation of the output power value was $\pm$ 14 W owing to the fluctuations in power at the laser source. The periodic water cooling led to changes in the laser temperature, which affected the output power. Throughout the testing process, the Nested HC-ARF was not damaged. The measurement time was limited by the water cooler that was used to cool the power meter, whose cooling capacity was less than the output power of the laser, thereby preventing long-term monitoring. When the lenses reached thermal stability, high-power laser transmission was achieved for a long period with constant transmission efficiency. Therefore, the results verify that the device can achieve high power and efficiency with stable transmission over long periods.

Hollow-core fibers exhibit lower nonlinearity than solid-core fibers owing to their air-guidance properties, making them suitable for high-power and narrow-linewidth laser transmission. To verify the low nonlinear transmission characteristics of the Nested HC-ARF, we used a 110 m long fiber for high-power transmission with a final output power of 2850 W and a transmission efficiency of 91.8% at a bend radius of 30 cm. By comparing the difference in transmission efficiency of 10 m and 110 m long fibers at this bend radius, it can be inferred that the fabricated multimode Nested HC-ARF had a lower transmission loss of 1.6 dB/km at a bending radius of 30 cm. The loss value is lower than the previously cutback measured value. We attribute this to two reasons. One is that the looser coiling avoids light loss due to extrusion and tension. The second is that larger bending radius results in less bending loss. For this type of Nested HC-ARF, the bending performance is optimized, but additional optical leakage still occurs at small bending radius due to the relatively large core to wavelength ratio [6]. The spectral shape was evaluated at the highest output power for fiber transmission lengths of 10 and 110 m and compared with the output spectral shape of the laser (Fig. 6). The comparison indicated a good agreement between the three spectra. Thus, no nonlinear effects were observed for either length after Nested HC-ARF transmission, verifying the low nonlinearity of this approach.

IV. Conclusion

In this study, we designed and fabricated a low-loss multimode 8-tube Nested HC-ARF. On this basis, we experimentally verified the transmission of 3 kW power through a 10 m long low-loss multi-mode Nested HC-ARF with a transmission efficiency of 95.2%. To the best of our knowledge, these are the highest values reported for output power through HC-ARF. Meanwhile, the beam quality and spectrum were found to be in good agreement with the laser source. No nonlinearities were observed at the transmission lengths of 10 and 110 m. Additionally, the high-power transmission system based on the fabricated multimode Nested HC-ARF can be expanded further to higher power levels, paving the way for the development of next-generation high-power few- or multi-mode laser transmission systems. In future studies, the micro-bending loss mechanism of multimode HC-ARF will be explored to optimize the fiber structure design. Meanwhile, transmission power will be increased, leading to miniaturization and integration of the transmission system. We believe these systems may have wide applications in industrial processing, materials processing, laser medicine, and defense technologies.

References

[1] M. Naeem, "Advances in drilling with fiber lasers," *Proc. SPIE.*, vol. 9657, pp. 24–33, 2015.
[2] Z. Qu, Q. Li, H. Meng, X. Sui, H. Zhang, and X. Zhai, "Application and the key technology on high-power fiber-optic laser in laser weapon," *Proc. SPIE*, vol. 9294, pp. 65–69, 2014.
[3] E. Stiles, "Proceedings of the 5th international workshop on fiber lasers," in *Proc. 5th Int. Workshop Fiber Lasers*, 2009, p. 4.
[4] T. Matsui et al., "Effective area enlarged photonic crystal fiber with quasi-uniform air-hole structure for high power transmission," *Inst. Elect., Inf. Commun. Engineers Trans. Commun.*, vol. 103, no. 4, pp. 415–421, 2020, doi: 10.1587/transcom.2019EBP3100.
[5] T. Okuda, Y. Fujiya, S. Goya, and A. Inoue, "Beam transmission technology by photonic crystal fiber to realizes high-precision and high-efficiency laser processing technology," *Mitsubishi Heavy Industries Tech. Rev.*, vol. 57, pp. 1–5, 2020.
[6] W. Shere, E. N. Fokoua, G. T. Jasion, and F. Poletti, "Designing multi-mode anti-resonant hollow-core fibers for industrial laser power delivery," *Opt. Exp.*, vol. 30, no. 22, pp. 40425–40440, Oct. 2022, doi: 10.1364/OE.473681.
[7] A. N. Kolyadin et al., "negative curvature hollow-core fibers: Dispersion properties and femtosecond pulse delivery," *Phys. Procedia*, vol. 73, pp. 59–66, 2015, doi: 10.1016/j.phpro.2015.09.122.

[8] G. P. Agrawal, "Applications of nonlinear fiber optics," Academic, London, U.K., 2020.

[9] R. F. Cregan et al., "Single-mode photonic band gap guidance of light in air," *Science*, vol. 285, no. 5433, pp. 1537–1539, Sep. 1999, doi: 10.1126/science.285.5433.1537.

[10] Y. Y. Wang, N. V. Wheeler, F. Couny, P. J. Roberts, and F. Benabid, "Low loss broadband transmission in hypocycloid-core Kagome hollow-core photonic crystal fiber," *Opt. Lett.*, vol. 36, no. 5, pp. 669–671, Mar. 2011, doi: 10.1364/OL.36.000669.

[11] W. Belardi and J. C. Knight, "Hollow antiresonant fibers with reduced attenuation," *Opt. Lett.*, vol. 39, no. 7, pp. 1853–1856, Apr. 2014, doi: 10.1364/OL.39.001853.

[12] F. Poletti, "Nested antiresonant nodeless hollow core fiber," *Opt. Exp.*, vol. 22, no. 20, pp. 23807–23828, Oct. 2014, doi: 10.1364/OE.22.023807.

[13] B. Debord et al., "Ultralow transmission loss in inhibited-coupling guiding hollow fibers," *Optica*, vol. 4, no. 2, pp. 209–217, 2017, doi: 10.1364/optica.4.000209.

[14] F. Yu, P. Song, D. Wu, T. Birks, D. Bird, and J. Knight, "Attenuation limit of silica-based hollow-core fiber at mid-IR wavelengths," *Appl. Phys. Lett. Photon.*, vol. 4, no. 8, 2019, Art. no. 080803, doi: 10.1063/1.5115328.

[15] P. Roberts et al., "Achieving low loss and low nonlinearity in hollow core photonic crystal fibers," in *Proc. Conf. Lasers Electro-Opt.*, 2005, Paper CWA7.

[16] J. D. Shephard, F. Couny, P. S. Russell, J. D. Jones, J. C. Knight, and D. P. Hand, "Improved hollow-core photonic crystal fiber design for delivery of nanosecond pulses in laser micromachining applications," *Appl. Opt.*, vol. 44, no. 21, pp. 4582–4588, Jul. 2005, doi: 10.1364/ao.44.004582.

[17] S. F. Gao et al., "Hollow-core conjoined-tube negative-curvature fibre with ultralow loss," *Nature Commun.*, vol. 9, no. 1, Jul. 2018, Art. no. 2828, doi: 10.1038/s41467-018-05225-1.

[18] S. F. Gao, Y. Y. Wang, W. Ding, Y. F. Hong, and P. Wang, "Conquering the Rayleigh scattering limit of silica glass fiber at visible wavelengths with a hollow-core fiber approach," *Laser Photon. Rev.*, vol. 14, no. 1, 2019, Art. no. 1900241, doi: 10.1002/lpor.201900241.

[19] H. Sakr et al., "Hollow core optical fibres with comparable attenuation to silica fibres between 600 and 1100 nm," *Nature Commun.*, vol. 11, no. 1, Nov. 2020, Art. no. 6030, doi: 10.1038/s41467-020-19910-7.

[20] X. Zhang et al., "Low loss nested hollow-core anti-resonant fiber at 2 microm spectral range," *Opt. Lett.*, vol. 47, no. 3, pp. 589–592, Feb. 2022, doi: 10.1364/OL.447418.

[21] G. T. Jasion et al., "0.174 dB/km hollow core double nested antiresonant nodeless fiber (DNANF)," in *Proc. IEEE Opt. Fiber Commun. Conf. Exhib.*, 2022, pp. 1–3.

[22] H. C. H. Mulvad et al., "Kilowatt-average-power single-mode laser light transmission over kilometre-scale hollow-core fibre," *Nature Photon.*, vol. 16, no. 6, pp. 448–453, 2022, doi: 10.1038/s41566-022-01000-3.

[23] M. A. Cooper et al., "2.2 kW single-mode narrow-linewidth laser delivery through a hollow-core fiber," *Optica*, vol. 10, no. 10, pp. 1253–1259, 2023, doi: 10.1364/optica.495806.

[24] C. Dumitrache, J. Rath, and A. P. Yalin, "High power spark delivery system using hollow core Kagome lattice fibers," *Materials*, vol. 7, no. 8, pp. 5700–5710, Aug. 2014, doi: 10.3390/ma7085700.

[25] B. Debord et al., "Multi-meter fiber-delivery and pulse self-compression of milli-Joule femtosecond laser and fiber-aided laser-micromachining," *Opt. Exp.*, vol. 22, no. 9, pp. 10735–10746, May 2014, doi: 10.1364/OE.22.010735.

[26] U. Brauch, C. Röcker, T. Graf, and M. Abdou Ahmed, "High-power, high-brightness solid-state laser architectures and their characteristics," *Appl. Phys. B*, vol. 128, no. 3, 2022, Art. no. 58, doi: 10.1007/s00340-021-07736-0.

[27] P. Uebel et al., "Broadband robustly single-mode hollow-core PCF by resonant filtering of higher-order modes," *Opt. Lett.*, vol. 41, no. 9, pp. 1961–1964, May 2016, doi: 10.1364/OL.41.001961.

[28] H. Sakr et al., "Hollow core NANFs with five nested tubes and record low loss at 850, 1060, 1300 and 1625 nm," in *Proc. Opt. Fiber Commun. Conf.*, 2021, Paper F3A–F34.

[29] W. Shere, G. T. Jasion, E. N. Fokoua, and F. Poletti, "Design rules for multi-mode anti-resonant hollow-core fibres," in *Proc. Opt. Fiber Commun. Conf.*, 2021, Paper F4C–F44.

[30] C. Goel and S. Yoo, "Multimode nested antiresonant hollow core fiber," *J. Lightw. Technol.*, vol. 39, no. 20, pp. 6592–6598, Oct. 2021, doi: 10.1109/jlt.2021.3101522.

[31] M. Petry, C. Markos, R. A. Correa, and M. S. Habib, "Multi-mode guidance in enhanced inhibited coupling hollow-core anti-resonant fibers," in *Proc. Conf. Lasers Electro-Opt. Sci. Innov.*, 2022, Paper JTh3B.42.

[32] B. Winter, T. A. Birks, and W. J. Wadsworth, "Multimode hollow-core anti-resonant optical fibres," in *Proc. Front. Opt.*, 2019, Paper JTu4A-18.

[33] Z. Dong, X. Zhang, P. Yao, J. Yao, S. Wan, and P. Wang, "Development of multi-mode rod-type hollow-core antiresonant fiber," *Proc. SPIE*, vol. 12280, pp. 25–31, 2022.

[34] D. Wu et al., "Low-loss multi-mode anti-resonant hollow-core fibers," *Opt. Exp.*, vol. 31, no. 13, pp. 21870–21880, Jun. 2023, doi: 10.1364/OE.492787.

[35] F. Abt, A. Heß, and F. Dausinger, "Focusing of high power single mode laser beams," in *Proc. Int. Congr. Appl. Lasers Electro-Opt.*, 2007, pp. 77–82.

[36] V. Zuba et al., "Limits of coupling efficiency into hollow-core antiresonant fibres," *J. Lightw. Technol.*, vol. 41, no. 19, pp. 6374–6382, Oct. 2023, doi: 10.1109/jlt.2023.3279701.

[37] S. Selleri, L. Vincetti, A. Cucinotta, M. J. O. Zoboli, and Q. Electronics, "Complex FEM modal solver of optical waveguides with PML boundary conditions," *Opt. Quantum Electron.*, vol. 33, pp. 359–371, 2001.

[38] J.-P. Negel et al., "Delivery of 800 W of nearly diffraction-limited laser power through a 100 m long multi-mode fiber," *Laser Phys. Lett.*, vol. 11, no. 5, 2014, Art. no. 055104, doi: 10.1088/1612-2011/11/5/055104.

[39] J. W. Nicholson, A. D. Yablon, S. Ramachandran, and S. Ghalmi, "Spatially and spectrally resolved imaging of modal content in large-mode-area fibers," *Opt. Exp.*, vol. 16, no. 10, pp. 7233–7243, 2008, doi: 10.1364/oe.16.007233.